

Supporting Information

Tuning Exchange Coupling in NiO-Based Bimagnetic Heterostructured Nanocrystals

Abdullah Al Shafe^{1†}, Mohammad Delower Hossain², Robert A. Mayanovic^{1*}, Vladimir Roddatis³, Mourad Benamara⁴

¹ Department of Physics, Astronomy and Materials Science, Missouri State University, Springfield, MO 65897, USA

² Department of Materials Science and Engineering, The Pennsylvania State University, University Park, PA 16802, USA

³ GFZ German Research Centre for Geosciences, Telegrafenberg, 14473 Potsdam, Germany

⁴ University of Arkansas Nano-Bio Materials Characterization Facility, University of Arkansas, Fayetteville, AR 72701, USA

*Email: RobertMayanovic@MissouriState.edu

†Department of Materials Science and Engineering, North Carolina State University, Raleigh, NC 27695, USA.

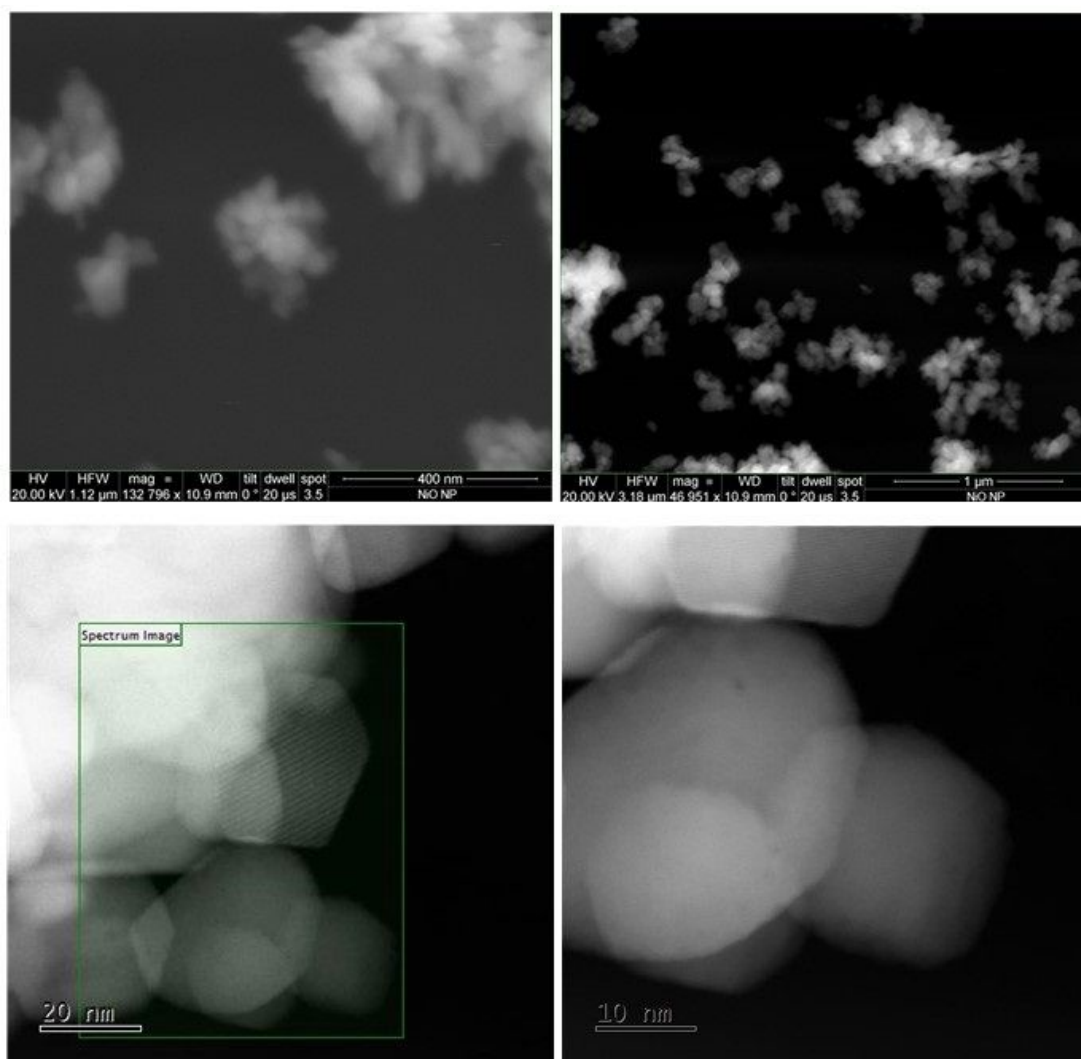


Figure S1: SEM images of NiO nanoparticles at different resolutions (top panels), High resolution TEM images (lower panels) of the NiO nanoparticles showing no trace of overgrowth.

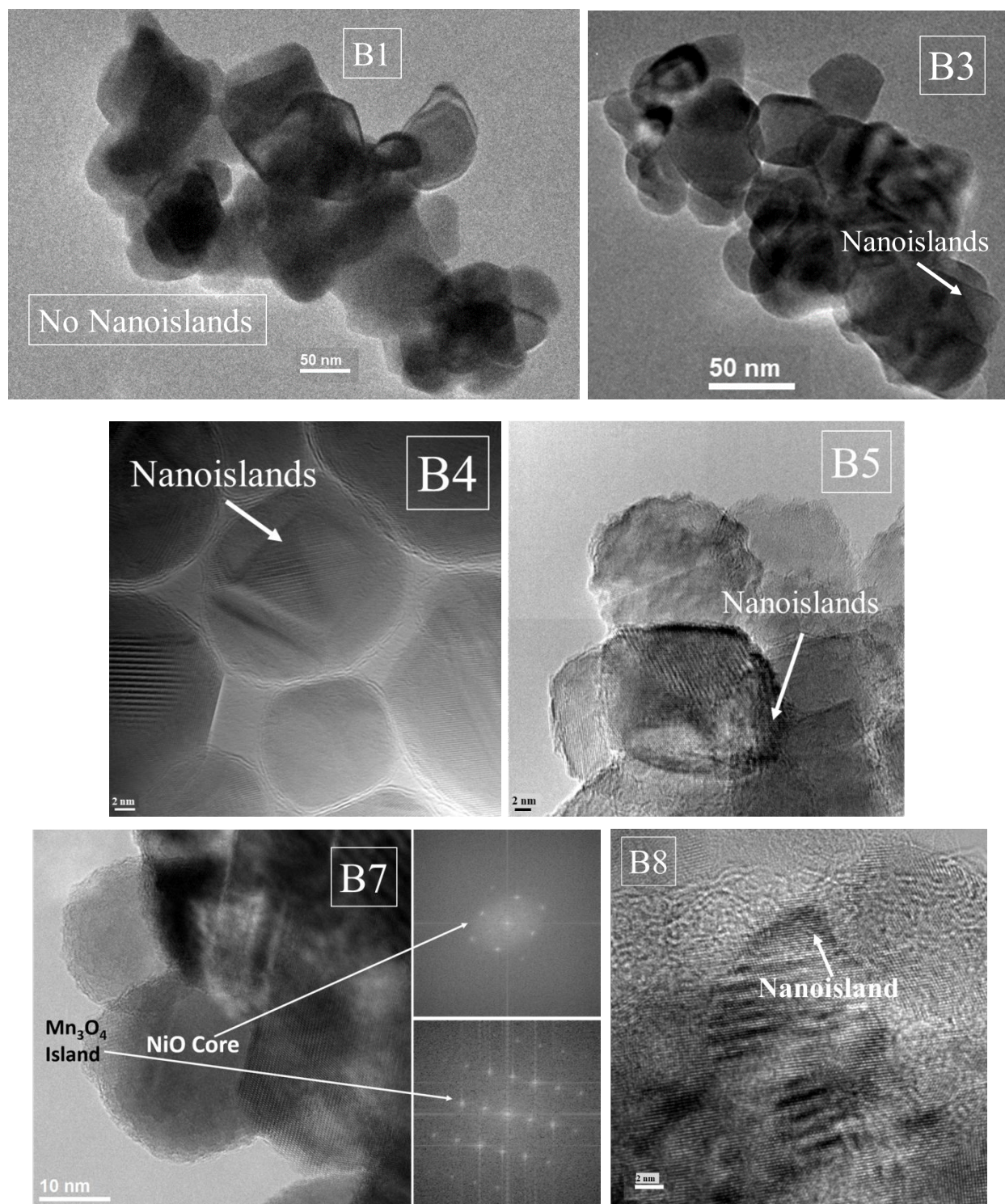


Figure S2: Additional TEM images of select samples B1, B3, B4, B5, B7 and B8, showing overgrowth morphologies or lack thereof. Also shown are the FFT of the NiO core region (top panel) and of the Mn_3O_4 island region (bottom panel) of an isolated B7 nanocrystal, just to the right of the high resolution TEM image of the same nanocrystal.

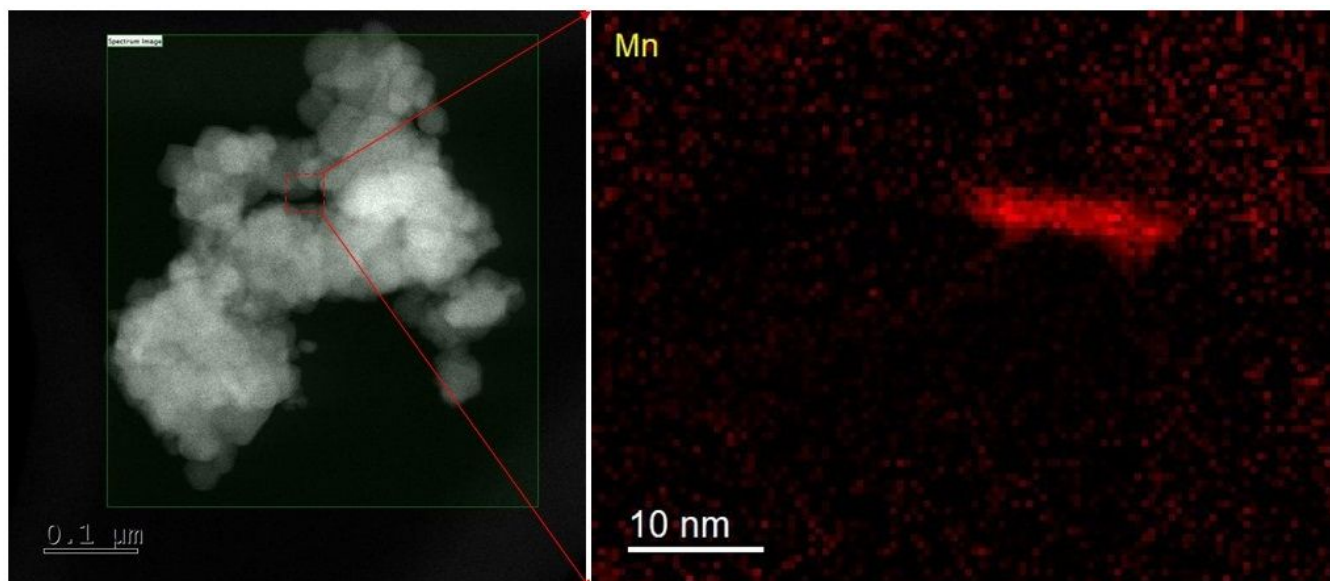


Figure S3: An HAADF image of sample B1 (left panel) and a TEM-EELS Mn (in red) elemental map (right panel) of the region outlined in the rectangle in the left panel. These are also shown in Figure 3 and are shown here for better clarity.

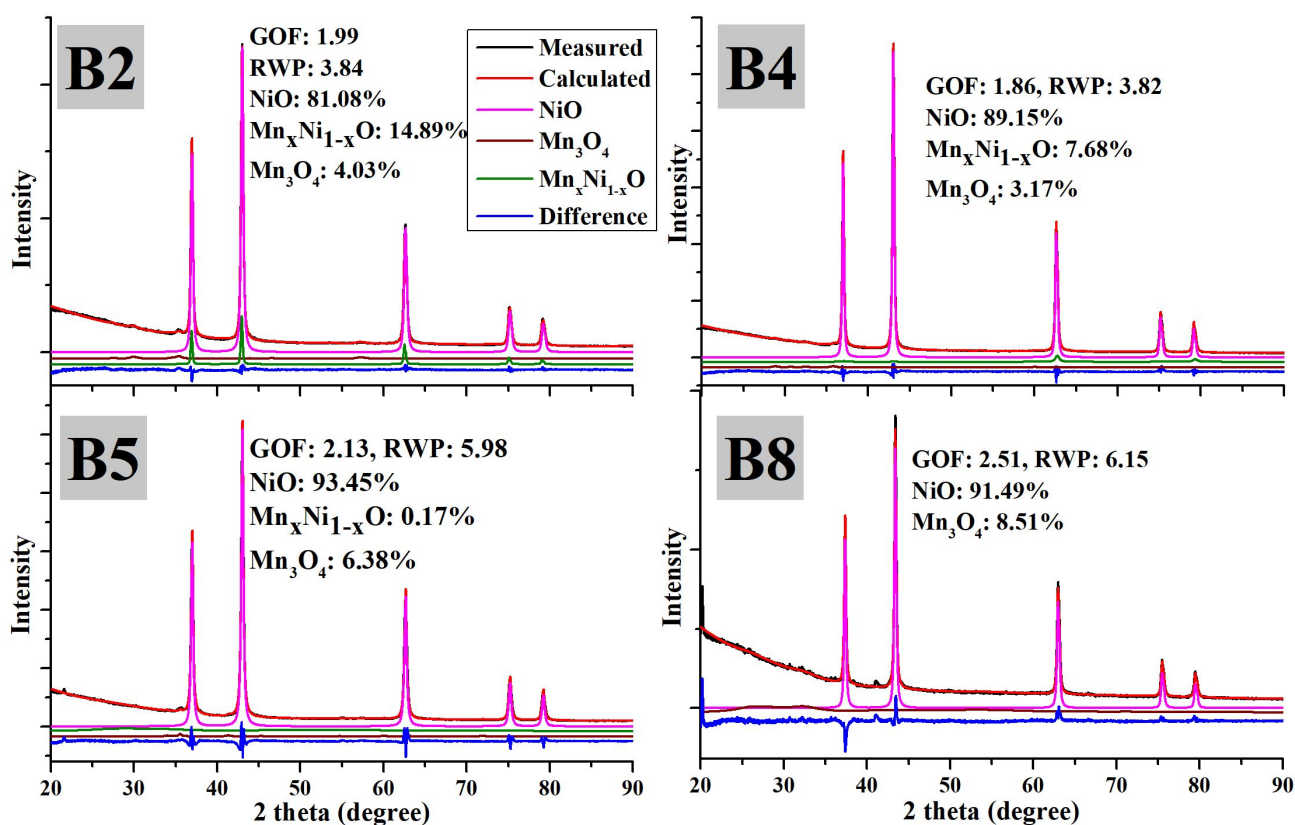


Figure S4: The Rietveld refinement fitting of the XRD data measured from the MHNC samples B2 (pH = 3.0), B4 (pH = 4.0), B5 (pH = 4.5) and B8 (pH = 7.0).

Table S1: Summary of structural results obtained from Rietveld refinement of the XRD data measured from samples B1 to B8. GOF is goodness of fit parameter and R_{WP} is the weighted profile R-factor.

Sample	NiO (%at)	$Mn_xNi_{1-x}O$ (%at)	Mn_3O_4 (%at)	$a(\text{\AA})$ NiO	$a(\text{\AA})$ $Mn_xNi_{1-x}O$	Mn_3O_4		GOF	R_{WP}
						$a(\text{\AA})$	$c(\text{\AA})$		
B1	96.51	3.49	0	4.176	4.183	0	0	1.91	3.53
B2	81.08	14.89	4.03	4.175	4.179	5.83	9.89	1.99	3.84
B3	75.97	22.00	2.02	4.174	4.179	5.78	10.25	1.79	3.42
B4	89.31	7.68	3.02	4.174	4.181	5.79	10.03	1.86	3.82
B5	93.45	0.17	6.38	4.175	0	5.89	9.80	2.13	5.98
B6	89.75	0	10.25	4.175	0	5.77	9.51	1.66	3.36
B7	92.57	0	7.43	4.174	0	5.84	9.56	1.96	3.92
B8	91.49	0	8.51	4.178	0	5.80	9.56	2.51	6.15

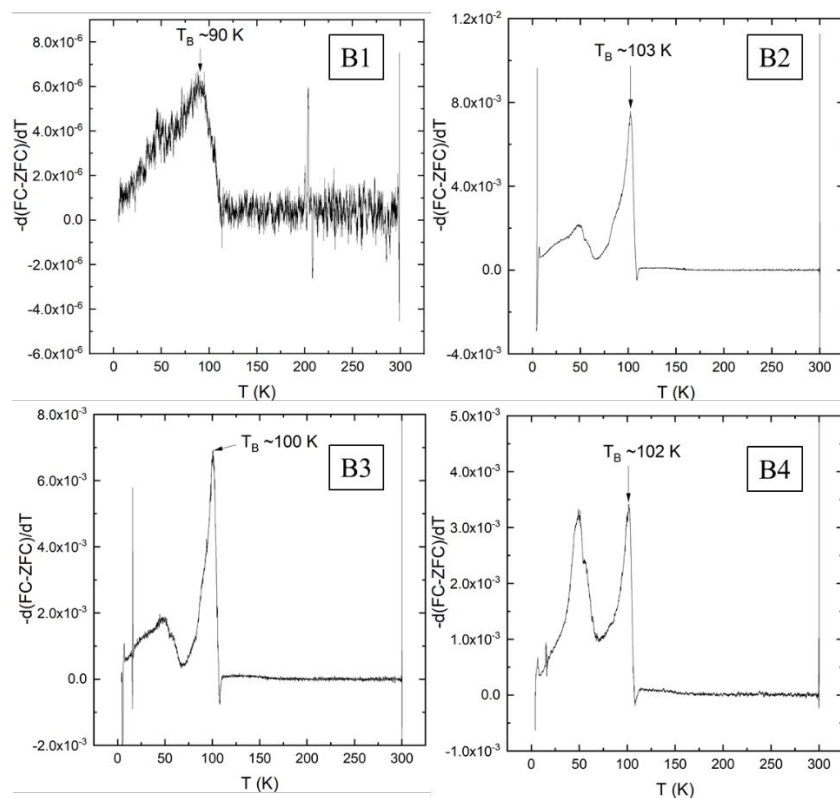


Figure S5: Curves used to determine the blocking temperatures from the magnetization vs temperature data measured from MHNC samples B1 (top left; pH = 2.4), B2 (top right; pH = 3), B3 (bottom left; pH = 3.5) and B4 (bottom right; pH = 4.0).

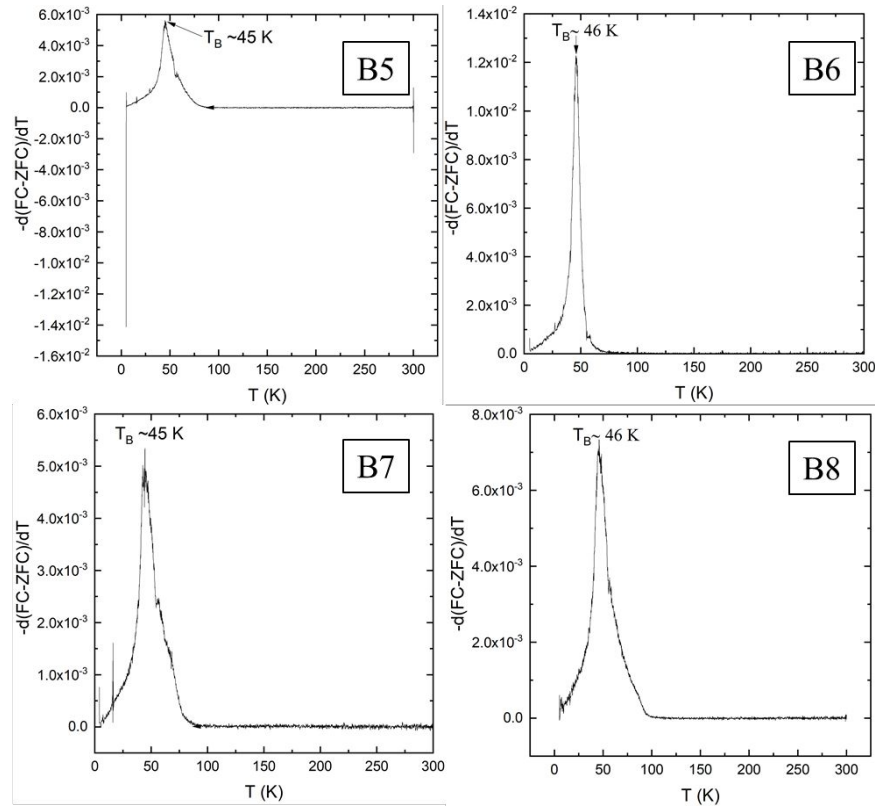


Figure S6: Curves used to determine the Blocking temperatures from the magnetization vs temperature data measured from MHNC samples B5 (top left; pH = 4.5), B6 (top right; pH = 5.0), B7 (bottom left; pH = 6.0) and B8 (bottom right; pH = 7.0).

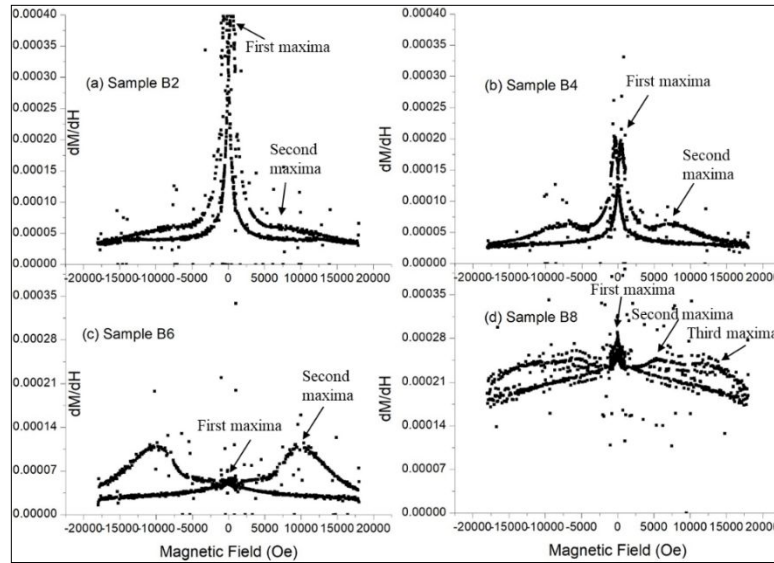


Figure S7: The derivative of magnetization as a function of applied magnetic field (i.e., susceptibility) vs magnetic field of (a) sample B2, (b) sample B4, (c) sample B6, and (d) sample B8.

Figure S5 shows the susceptibility vs magnetic field (H) data for select samples, where the susceptibility was calculated as a dM/dH derivative of the M vs H data. The maxima of the susceptibility data indicate the magnetization reversal of the phases present in the MHNCs.¹ The susceptibility data for samples B1 and B2 do not show prominent second maxima whereas the data for the remainder of the samples have at least one additional set of maxima. We conjecture that the principal maxima (peaks near ~ 500 Oe) coincide with NiO-core- $Mn_xNi_{1-x}O$ -shell spin-spin interactions whereas the second maxima coincide with NiO-core- Mn_3O_4 -island spin-spin interactions. This is consistent with the reduction of the first maxima, coinciding with

the reduction of the $\text{Mn}_x\text{Ni}_{1-x}\text{O}$ shell nanophase, and the general increase of the higher-order maxima, coinciding with the emerging predominance of the decorating Mn_3O_4 islands, with increasing pH used to synthesize samples B1 to B8. The third maxima in B8 may result from the unknown phase(s).

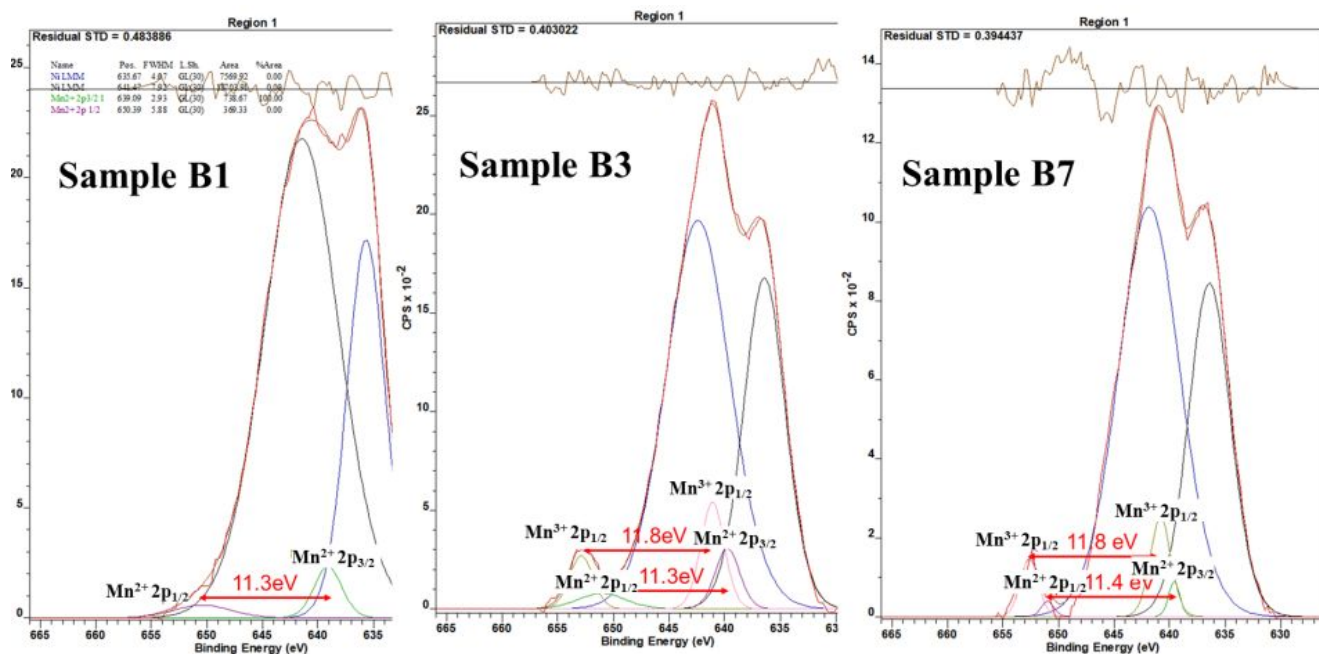


Figure S8: Mn 2p XPS spectra of different nanocrystal samples showing the binding energy difference of Mn 2p_{1/2} and 2p_{3/2} peaks.

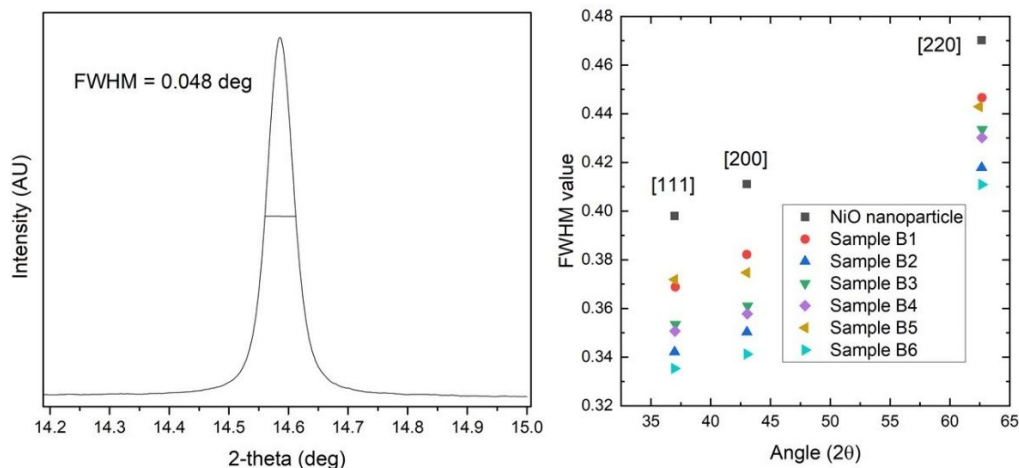


Figure S9: FWHM value of the standard CeO_2 NIST sample (left panel), FWHM values at different peak positions of other nanocrystal samples including the NiO nanoparticle (right panel).

REFERENCES

(1) Fontañña Troitiño, N.; Rivas-Murias, B.; Rodríguez-González, B.; Salgueiriño, V. Exchange Bias Effect in $\text{CoO@Fe}_3\text{O}_4$ Core-Shell Octahedron-Shaped Nanoparticles. *Chem. Mater.* **2014**, *26* (19), 5566–5575. <https://doi.org/10.1021/cm501951u>.